

# Training Robots without Robots: Deep Imitation Learning for Master-to-Robot Policy Transfer

Heecheol Kim<sup>1,3</sup>, Yoshiyuki Ohmura<sup>1</sup>, Akihiko Nagakubo<sup>2</sup>, and Yasuo Kuniyoshi<sup>1</sup>

**Abstract**—Deep imitation learning is a promising method for dexterous robot manipulation because it only requires demonstration samples for learning manipulation skills. In this paper, deep imitation learning is applied to tasks that require force feedback, such as bottle opening. However, simple visual feedback systems, such as teleoperation, cannot be applied because they do not provide force feedback to operators. Bilateral teleoperation has been used for demonstration with force feedback; however, this requires an expensive and complex bilateral robot system. In this paper, a new master-to-robot (M2R) transfer learning system is presented that does not require robots but can still teach dexterous force feedback-based manipulation tasks to robots. The human directly demonstrates a task using a low-cost controller that resembles the kinematic parameters of the robot arm. Using this controller, the operator can naturally feel the force feedback without any expensive bilateral system. Furthermore, the M2R transfer system can overcome domain gaps between the master and robot using the gaze-based imitation learning framework and a simple calibration method. To demonstrate this, the proposed system was evaluated on a bottle-cap-opening task that requires force feedback only for the master demonstration.

**Index Terms**—Imitation Learning, Deep Learning in Grasping and Manipulation, Grippers and Other End-Effectors, Force and Tactile Sensing, Dual Arm Manipulation

## I. INTRODUCTION

Deep imitation learning is a model-free method for policy optimization that imitates expert (typically, human) demonstrated behaviors using a deep neural network. Because this method can learn an arbitrary policy without a handcrafted model for an environment or object, it has been applied to dexterous robot manipulation tasks for which the manual definition of the optimal solution is infeasible (e.g., [1], [2], [3]).

The aim of this study is the imitation learning of a manipulation task that requires force feedback for successful manipulation. Previous demonstration methods for imitation learning suffer when they consider force feedback. First, in teleoperation-based methods where the human operator teleoperates the robot using the controller (e.g., [3], [4]),

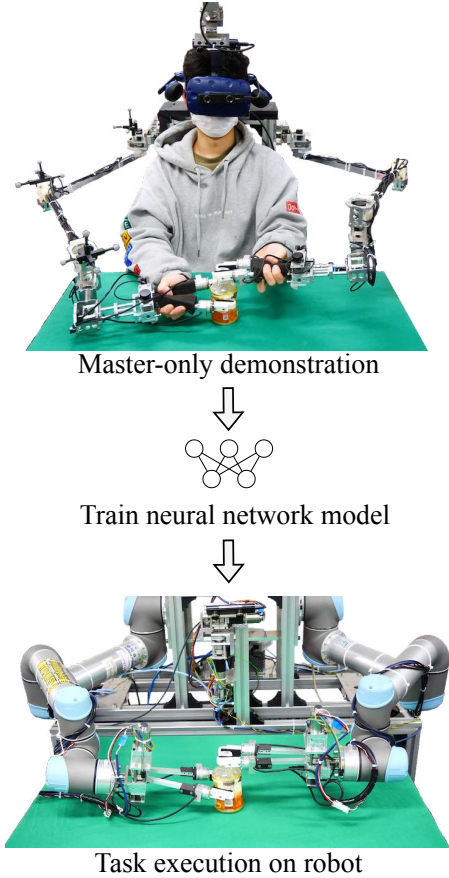


Fig. 1: Master-to-robot (M2R) transfer learning system can teach a robot from master-only-generated demonstrations. For example, the trained neural network model can successfully execute a bottle-cap-opening task that requires force feedback on real robots (UR5).

force feedback is not provided to the human operator. Second, bilateral teleoperation enables accurate force control by reproducing the force feedback of the robot to the master's actuators (e.g., [5], [6], [7]). However, this method requires a complex control rule to compensate for the time delay caused by communication between the master and robot [8], is expensive because both the master and robot require a motor, and the safety of the human operator who physically interacts with the moving actuators must be considered [5]. Third, kinesthetic teaching is another robot teaching method in which a human grasps the robot arm and teaches the task by moving it (e.g., [9], [10], [11]). However, when adapting

<sup>1</sup> Laboratory for Intelligent Systems and Informatics, Graduate School of Information Science and Technology, The University of Tokyo, 7-3-1 Hongo, Bunkyo-ku, Tokyo, Japan (e-mail: {h-kim, ohmura, kuniyoshi}@isi.imi.i.u-tokyo.ac.jp, Fax: +81-3-5841-6314).

<sup>2</sup> Artificial Intelligence Research Center, National Institute of Advanced Industrial Science and Technology, 1-1-1 Umezono, Tsukuba, Ibaraki, Japan (e-mail: nagakubo.a@aist.go.jp).

<sup>3</sup> Corresponding author

This paper was supported in part by the Department of Social Cooperation Program "Intelligent Mobility Society Design," funded by Toyota Central R&D Labs., Inc., of the Next Generation AI Research Center, The University of Tokyo.

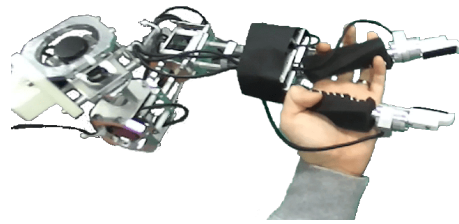
the method to the end-to-end learning of visuomotor control, this method suffers from severe visual distractions, such as the human body. Additionally, this method requires a torque sensor on each joint for gravity and friction compensation; therefore, a high-cost force controllable robot is required. Finally, a few researchers have studied a robot that *learns from watching* humans demonstrate tasks [12], [13], [14], [15]. However, these methods cannot transfer force feedback because it cannot be acquired from video demonstrations. To summarize, current demonstration generation methods lack force feedback or require expensive robots in the demonstration system. This problem raises the demand for a simple demonstration method that can be applied to force feedback-based tasks.

In this study, a simple master-only demonstration system that can imitate tasks that require force feedback (Fig. 1) is proposed. This system must overcome two types of domain gaps between the master and robot: visual gap and kinematic gap. The visual gap is a domain gap in vision caused by different visual components, such as the human arm. A hand-in-camera type of controller can minimize this gap [16]. However, this hand-in-camera setup is only valid for tasks that do not require global vision, such as pick-and-place. Therefore, human-like dual-arm dexterous manipulation considering the entire scene is not feasible with the hand-in-camera setup. Gaze-based deep imitation learning [4] was proposed, which can suppress the visual gap using the human gaze naturally estimated during the demonstration. Because the human gaze naturally foveates on the target object [17], foveated vision cropped from global vision using the predicted gaze position effectively suppresses the visual gap.

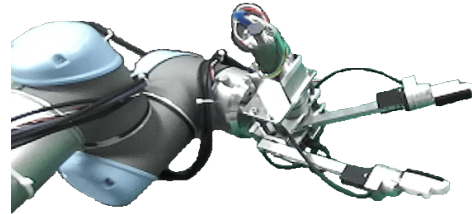
The kinematic gap is a domain gap between the master controller and robot caused by their kinematic difference. To solve this, in this study, a master controller is designed that imitates the same Denavit–Hartenberg (DH) parameters as the UR5 (Universal Robots) robot, and the robot and controller share the same end-effector design. The human demonstrator uses this controller to directly manipulate the object. Therefore, the human can naturally feel force feedback during manipulation. Additionally, a simple calibration method is used to minimize the kinematic gap.

This master controller for M2R transfer has a few advantages. First, demonstration with force feedback is possible because a human directly manipulates objects. Second, this controller can teach tasks that require force feedback without an expensive bilateral system; this controller does not require any motor or gear, only a simple encoder. Finally, this system is scalable because no robot is required during training [18]; a large-scale demonstration can be achieved by multiple master-only systems, which are cheaper than robot systems.

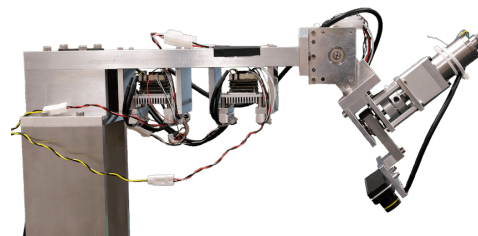
The proposed gaze-based dual-action (DA) imitation learning method, accompanied by a master-only demonstration system, is validated in the real-world robot experiment of a bottle-cap-opening task, which requires both a precise grasping-cap policy, and the policy considers force feedback.



(a) Master controller and end-effector



(b) UR5 robot and end-effector



(c) Camera mount

Fig. 2: M2R transfer learning system. The master controller (2a) and robot (2b) share the same DH parameter, fingertip, and (2c) camera mount.

## II. METHOD

### A. Master-robot transfer learning system

The dual-arm robot system with UR5 is used. In the authors' previous research (e.g., [4]), this system was operated in teleoperation mode. In this study, by contrast, demonstration data are generated in master-only mode. In this mode, the human demonstrator grasps the master controller (Fig. 2a) and executes the task using its fingertip. The controller collects joint angles from its six-dimensional encoders mounted on a structure that has DH parameters identical to those of the UR5 robot. Therefore, the robot can easily reproduce human behavior by following the recorded encoder values. The end-effectors on the robot and master are identical, one degree-of-freedom (DoF) grippers (Fig. 2b). Additionally, a force/torque (F/T) sensor (Leptrino, PFS 030YA301) is placed between the fingertip and rod so that the F/T of the fingertip can be measured.

The human operator observes a stereo image from a stereo camera (ZED-Mini, StereoLabs) using a head-mounted display. The stereo cameras are mounted in identical relational positions on both the robot and master sides (Fig. 2c). For the master, this location is just above the operator's head. This shared camera mount position minimizes the visual gap between the master and robot caused by different viewpoints. The developed pan-tilt camera system can control its direc-

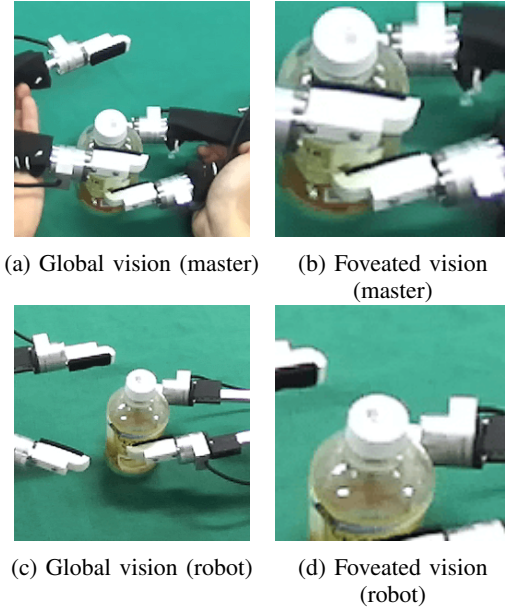


Fig. 3: Foveated vision can minimize the visual gap, such as the human hand.

tion, which can be used in future studies.

### B. Gaze prediction

A mixture density network (MDN)-based [19] gaze prediction architecture [20], [4] is used in this study to crop  $128 \times 128$  foveated vision from  $256 \times 256$  global vision (please see [4], [2] for details of the gaze predictor). To summarize, a series of five convolutional neural networks (CNNs) and rectified linear units (ReLU) followed by SpatialSoftmax [21] extracts visual features, which are then processed by the MDN, which is composed of a Gaussian mixture model (GMM) with eight Gaussians. Finally, this GMM is fitted to the coordinates of the gaze using [1]

$$\mathcal{L}_{gaze} = -\log\left(\sum_{i=1}^8 p^i \mathcal{N}(g; \mu^i, \Sigma^i)\right), \quad (1)$$

where  $p^i$ ,  $\mu^i$ , and  $\Sigma^i$  represent the weight, mean, and covariance matrix of the  $i$ th Gaussian, respectively, and  $g$  denotes the target gaze coordinate. Visual distractions, such as the human hand during demonstrations, are not included in the foveated vision (Fig. 3) because the human gaze is correlated with the target object position [17], [22]. Therefore, the visual appearance of both the robot and master are similar in the foveated vision.

### C. Network architecture

Because the cap-reaching behavior requires precise manipulation, the dual-action architecture proposed in [2] is used, which enables exact manipulation, such as needle threading. This architecture first detects if the end-effector is in foveated vision: if not, the global action, which is the fast action that delivers the hand to the vicinity of the target, is used; and if so, the local action, which is a precise and slow action when

the hand is near the target, is activated. Each step is labeled as  $\{global\ action, local\ action\}$  from the demonstration data and used to train the global-action network or local-action network, respectively. The details of the annotation are provided in III-A.1. Bottle cap opening is segmented into three subtasks (see Fig. 4):

- *GraspBottle*: grasp the body of the bottle using the right hand.
- *GraspCap*: reach and grasp the bottle cap with the left hand.
- *Rotate*: open the bottle cap by rotating the left hand.

Figure 5 illustrates three policy prediction architectures. First, the global-action network inputs the left (*GraspCap*) or right (*GraspBottle*) foveated images, robot state, and stereo gaze position to output the left-arm action (*GraspCap*) or right-arm action (*GraspBottle*). The action is defined by the difference between the seven-dimensional robot state (three-dimensional position, three-dimensional orientation, and a gripper angle) at the next step and the current robot state. The orientations of the robot state input into the neural network models are decomposed using cosine and sine to prevent a drastic change of the angle representation; therefore, it is ten-dimensional.

Second, the local-action network trains the local actions in *GraspCap*. This network only inputs foveated vision when the left end-effector is present to output the precise local action. Because the robot's kinematic state is not used for input, this network can accurately predict the action regardless of the kinematic gap between training data (master) and test environment (robot).

Finally, the *Rotate* network takes the dual-arm F/T sensory data and foveated image as input to perform *Rotate*. Because the authors of [1] proved that the Transformer-based self-attention architecture [23] reduces distractions in sensory input during the dual-arm task, this Transformer-based architecture is applied for F/T sensory input processing in this study.

The global-action and *Rotate* networks use a series of CNN, ReLU, and max-pooling layers with the stride equal to 2 (see [1] for details). The local-action network uses one CNN layer with ReLU followed by nine residual blocks [24], and a max-pooling layer is inserted in every two residual blocks of stride equal to 2. The CNN layer uses a  $3 \times 3$  filter with 32 channels. The multilayer perceptron (MLP) module is a series of fully connected layers (FCs) with a node size of 200 and ReLU between the FCs. Action is optimized with  $\ell_2$  loss.

### D. Calibration

The proposed controller and UR5 robot have identical DH parameters. However, the authors found that there is still an error because of the controller's low rigidity.

Motion capture is used for calibration. The accurate end-effector position and rotation are measured using the Optitrack motion capture device. The master controller is randomly moved by the human operator while it records the joint angle, and the motion capture device measures the exact



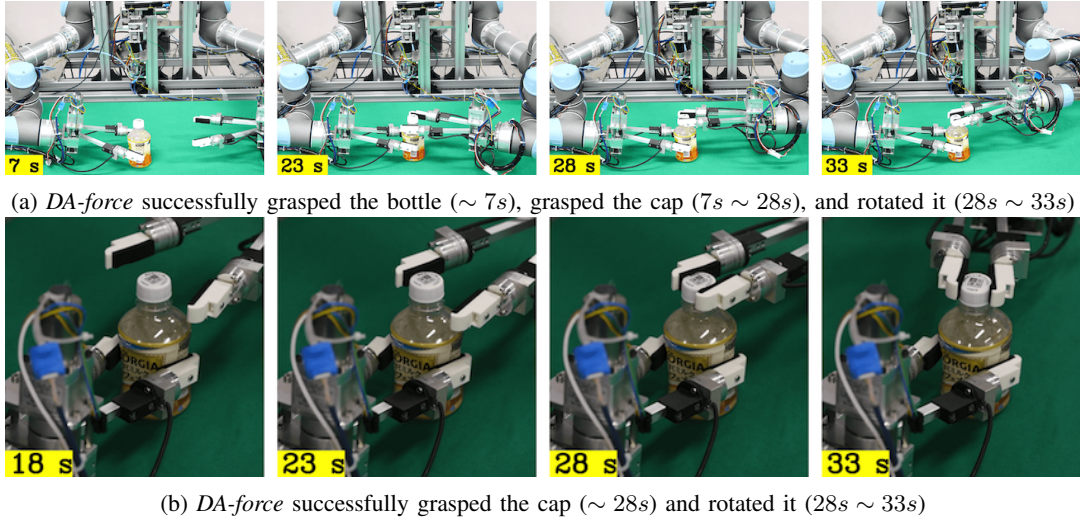


Fig. 4: Example of successful behavior of *DA-force*.

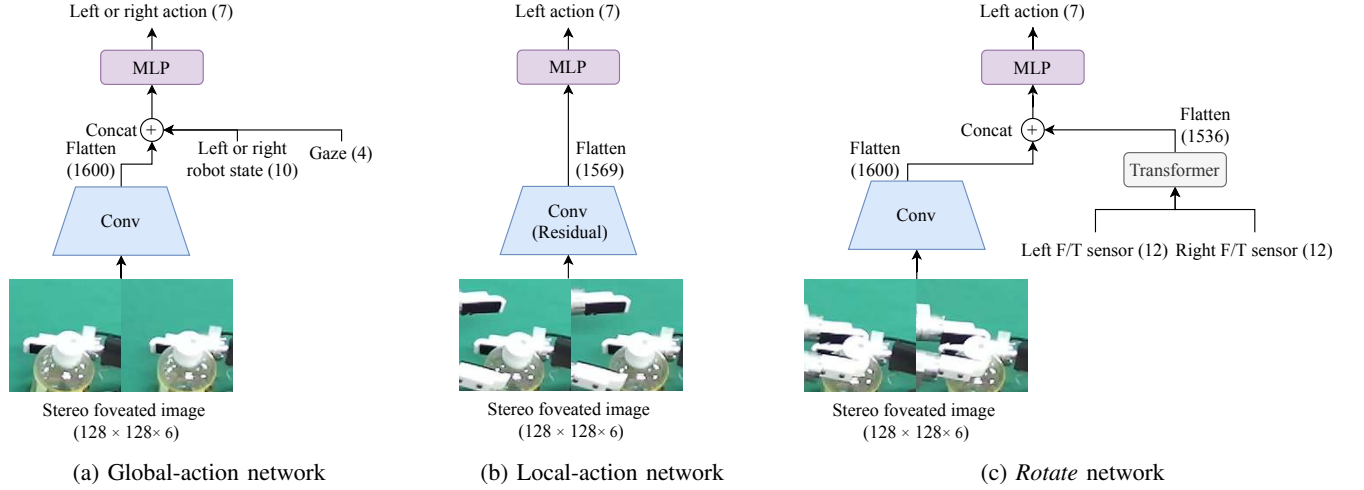


Fig. 5: Network architectures. The number in brackets indicates the dimensions of the data.

position simultaneously, which is then played back in the robot. A transformation from the motion-captured master position/rotation  $M_p^{mocap}$  to the robot position/rotation  $R_p^{mocap}$  transforms the position/rotation  $M_o^{enc}$  calculated from the joint angle into the calibrated robot state  $R_o^{enc}$ .

In this study, the position  $p$  and orientation  $o$  are separated, and the homogeneous transformation matrix  $A_p$  and rotation matrix  $A_o$  are calculated by learning the least-squares solution:

$$R_p^{mocap} = A_p^{4 \times 4} M_p^{mocap} \quad (2)$$

$$R_o^{mocap} = A_o^{3 \times 3} M_o^{mocap}. \quad (3)$$

Therefore, the calibration of robot state  $R^{enc}$  is calculated using the following equations:

$$R_p^{enc} = A_p^{4 \times 4} M_p^{enc} \quad (4)$$

$$R_o^{enc} = A_o^{3 \times 3} M_o^{enc}, \quad (5)$$

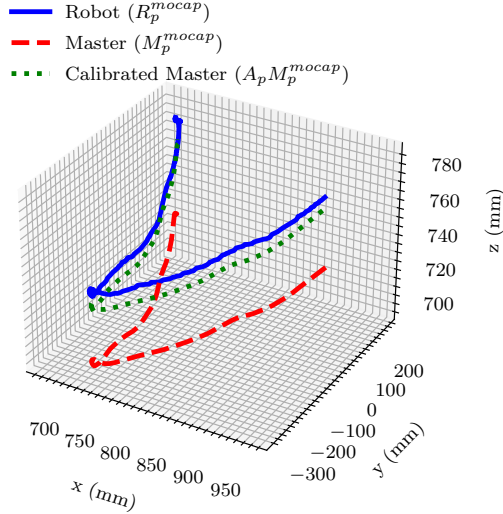
and the calibrated robot state  $R^{enc}$  is used for neural network model training.

Figure 6a illustrates part of the calibrated trajectory of the left arm. After calibration, the master controller's position  $M_p^{mocap}$  is translated into  $A_p M_p^{mocap}$ , which is much closer to the actual robot position  $R_p^{mocap}$ . Figure 6b compares the mean Euclidean distance between the master and robot,  $\|M_p^{mocap} - R_p^{mocap}\|$  (blue), and after calibration,  $\|A_p M_p^{mocap} - R_p^{mocap}\|$  (orange). The result indicates that the overall error decreases after calibration. Particularly, the error in the  $z$ -axis, which is mainly caused by the deformation of the upper arm because of gravity, occupies the most significant error between the master and robot, but can be decreased after calibration.

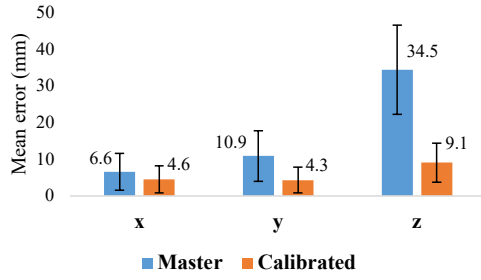
### III. EXPERIMENTS

#### A. Training setup

The proposed M2R transfer system was tested on the bottle-cap-opening task because this task requires precise reaching to the target and rotating the cap, which is only possible by rotating the gripper with the exact  $(x, y)$  transla-



(a) Visualized positions of part of the trajectory. Simple linear calibration can transform the master's trajectory into the robot's trajectory.



(b) Calibration reduces the kinematic error between the master and robot

Fig. 6: Calibration result.

Dataset	Number of demos	Total demo time (min)
<i>GraspBottle</i>	312	9.475
<i>GraspCap</i>	5798	156.0
<i>Rotate</i>	1111	23.75

TABLE I: Training dataset statistics.

tion to compensate for the offset between the cap and gripper. Even a human operator finds this behavior difficult without force feedback [25].

1) *Demonstration data generation*: During the demonstration, the human operator grasped the bottle with the right gripper (*GraspBottle*), reached the bottle cap with the left gripper (*GraspCap*), and repeatedly rotated the cap until it opened (*Rotate*). Each subtask was segmented during training using a foot keyboard. *GraspCap* was more complicated than the other two subtasks. Therefore, demonstrations that repeated *GraspCap* were added. The entire demonstration set was divided into 90% training and 10% validation sets. The training dataset statistics are presented in Table I.

From a  $1280 \times 720 \times 3$  raw RGB stereo camera image, a region of  $256 \times 256$  pixels was cropped around the center position of [678, 428] for left vision and [756, 428] for right

vision to reduce the visual gap.

The global/local action labels were annotated in *GraspCap*. First, a human manually annotated 202 demonstrations. The result labels were used to train a simple CNN-based binary classifier  $\pi(f_t) \rightarrow \{global\ action, local\ action\}$ , where  $f_t$  denotes the foveated image. The trained classifier then automatically classified the left demonstrations. If the classification result of one demonstration episode  $f_0, \dots, f_t$  provided more than one transition (i.e., annotation result showed  $\pi(f_{t-1}) \rightarrow local\ action$  and  $\pi(f_t) \rightarrow global\ action$  for any time step  $t \in [1, L]$ ), the human reannotated the demonstration episode.

2) *Model training*: The gaze predictor and policy network were trained on each subtask, respectively. Those models were trained for 300 epochs with a learning rate of  $3e-5$  using rectified Adam [26] and a weight decay of 0.01. For training, eight NVIDIA v100 GPUs with Intel Xeon CPU E5-2698 v4 or four NVIDIA a100 GPUs with two AMD EPYC 7402 CPUs were used, and for the robot tests, one NVIDIA GTX 1080 and one Intel i7-8700K CPU were used.

## B. Test setup

The objective of the test was to evaluate if the robot could grasp the bottle with its right hand, grasp the bottle cap with its left hand, and rotate the cap once without the cap slipping or bottle tilting. The test was repeated 18 times for different initial bottle positions, which were reproduced from the initial positions recorded in the randomly sampled validation set. The bottle cap was manually rotated approximately 90 degrees from the completed closed state because opening the completely locked cap required too much torque.

1) *Ablation study*: In this study, using the gaze-based dual-action approach with force feedback is proposed. Four types of neural network architecture were compared to evaluate the validity of each component:

- *DA-force*: *DA-force* use both F/T sensory feedback and gaze-based dual-action (DA) architecture.
- *No-force*: to validate the necessity of an F/T sensor, *No-force* does not input F/T sensor information while rotating the cap.
- *No-DA*: this architecture validates if dual-action is effective in the M2R framework. In this architecture, global action and local action are not distinguished. Therefore, the policy in each subtask is trained and inferred only from the global-action network.
- *No-gaze*: *DA-force* inputs foveated images to minimize the visual gap. *No-gaze* inputs global vision to investigate whether the visual gap is indeed reduced by gaze. As proposed in [3], the global image is processed using SpatialSoftmax after five layers of CNNs and ReLU.

## C. Experiment results

Figure 4 illustrates that the proposed *DA-force* successfully executed the bottle-cap-opening task. Among all the tested model architectures, *DA-force* had the best final accumulative success rate of 83.3% by combining DA, F/T sensor input, and gaze (Fig. 7).

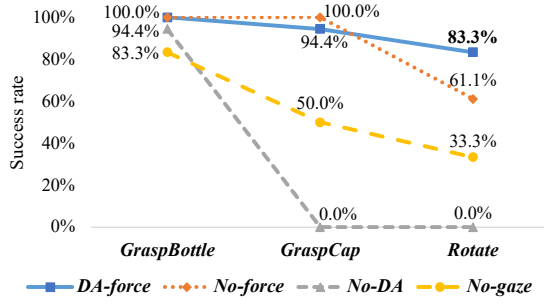


Fig. 7: Accumulative success rate (18 trials).

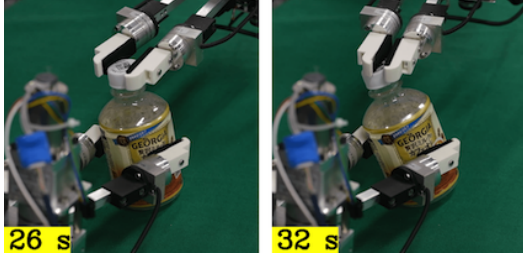


Fig. 8: Failure example of *No-force*. The fingertip slipped on the cap during rotation.

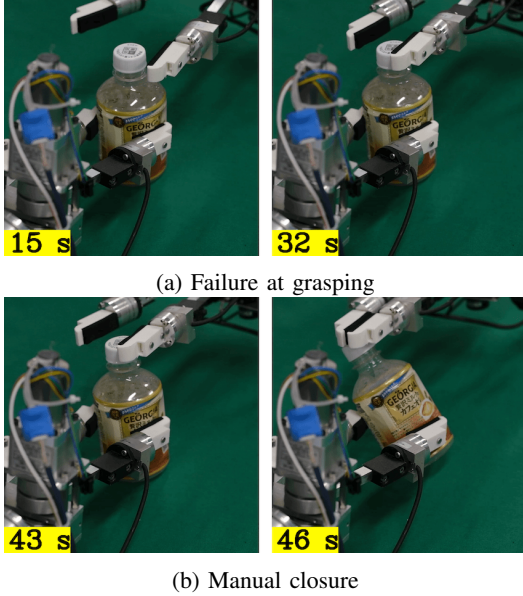


Fig. 9: Failure example of *No-DA*. The robot failed to grasp the bottle cap (9a). When the gripper was manually closed, the bottle collapsed (9b).

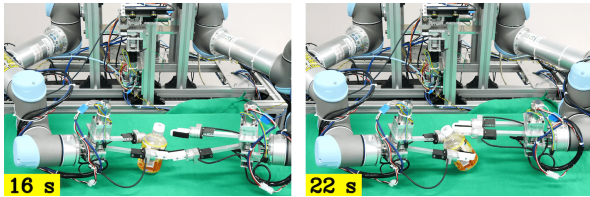


Fig. 10: Failure example of *No-gaze*. The robot was not able to correctly grasp the bottle cap.

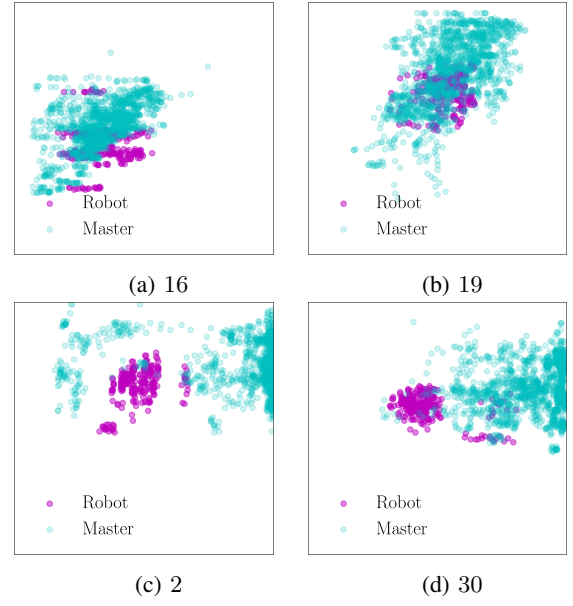


Fig. 11: Visualized SpatialSoftmax feature locations on the master (validation set) and robot (trials executed by *DA-force*). The number indicates the feature index (32 features total). Some features overlapped between the robot and master ((11a), (11b)), but other features predicted distinguished locations ((11c), (11d)), which caused a disparity of policy predictions.

*No-force*, which did not use F/T sensory information, executed accurate reaching and grasping, but poor manipulation during *Rotate* caused a slip during bottle cap opening (Fig. 8), which resulted in a lower final success rate than *DA-force*.

*No-DA* failed at accurately reaching the cap because it lacked the dual-action system (Fig. 9a). Some may argue that the gripper touched the bottle cap; therefore, simply closing it may lead to successful grasping. However, the bottle collapsed when the gripper was manually closed (Fig. 9b).

Finally, *No-gaze* demonstrated low accuracy for both *GraspBottle* and *GraspCap* (Fig. 10). This low accuracy was because the global vision-based policy was weak against distractions caused by the visual gap during M2R transfer. The visualized example of two-dimensional visual features extracted by SpatialSoftmax on the global vision processing network demonstrated the difference in the feature coordinates between the demonstration data collected by the master (validation set) and the robot data collected by *DA-force* during the test (Fig. 11). Some features focused on similar areas (Fig. 11a, 11b), whereas others focused on different areas (Fig. 11c, 11d). This difference resulted in errors in the action output computed from the MLP layer. Therefore the architecture using global vision failed to predict the accurate action.

#### IV. DISCUSSION

In this paper, a M2R dexterous manipulation skill transfer system using gaze-based dual-action deep imitation learning



was demonstrated. The proposed system was tested on the bottle-cap-opening task for a real robot. In this task, the demonstration dataset was generated only from the master. The proposed dual-action and gaze-based imitation learning method successfully learned bottle cap opening with an 83.3% success rate.

The proposed system has a few advantages over other robot teaching methods. First, this system does not require a robot during the demonstration. Because demonstration data collection and training are possible from a simple controller that consists of encoders and F/T sensors, this demonstration system is comparatively low-cost because no motors are required. Second, this M2R system can be efficiently scaled up. For example, a large-scale M2R system can consist of only one robot, and multiple masters can create large-scale demonstration data. Finally, this system can transfer policies that consider force feedback without a complex and expensive bilateral system. In this study, a one-DoF gripper was used. However, the proposed method is not limited to this specific gripper type. For example, [18] designed a multi-DoF mechanical glove that can also be used for the force feedback-based manipulation tasks in the present study.

The proposed method focused on learning a kinematic control policy using force feedback. This method provided sufficient manipulation skills for the bottle opening task; however, more dexterous manipulation tasks, such as fish filleting, require force control. In this case, a F/T sensory information-based impedance control method with torque-controllable robot manipulators will be required. This will be considered in future work.

## REFERENCES

- [1] H. Kim, Y. Ohmura, and Y. Kuniyoshi, "Transformer-based deep imitation learning for dual-arm robot manipulation," in *International Conference on Intelligent Robots and Systems*, 2021.
- [2] H. Kim, Y. Ohmura, and Y. Kuniyoshi, "Gaze-based dual resolution deep imitation learning for high-precision dexterous robot manipulation," *Robotics and Automation Letters*, pp. 1–1, 2021.
- [3] T. Zhang, Z. McCarthy, O. Jow, D. Lee, X. Chen, K. Goldberg, and P. Abbeel, "Deep imitation learning for complex manipulation tasks from virtual reality teleoperation," in *International Conference on Robotics and Automation*, 2018, pp. 1–8.
- [4] H. Kim, Y. Ohmura, and Y. Kuniyoshi, "Using human gaze to improve robustness against irrelevant objects in robot manipulation tasks," *Robotics and Automation Letters*, vol. 5, no. 3, pp. 4415–4422, 2020.
- [5] T. Hulin, K. Hertkorn, P. Kremer, S. Schätzle, J. Artigas, M. Sagardia, F. Zacharias, and C. Preusche, "The dlr bimanual haptic device with optimized workspace," in *International Conference on Robotics and Automation*, 2011, pp. 3441–3442.
- [6] A. Schiele and G. Hirzinger, "A new generation of ergonomic exoskeletons-the high-performance x-arm-2 for space robotics telepresence," in *International Conference on Intelligent Robots and Systems*, 2011, pp. 2158–2165.
- [7] J. Rebelo, T. Sednaoui, E. B. Den Exter, T. Krueger, and A. Schiele, "Bilateral robot teleoperation: A wearable arm exoskeleton featuring an intuitive user interface," *IEEE Robotics & Automation Magazine*, vol. 21, no. 4, pp. 62–69, 2014.
- [8] J. Guo, C. Liu, and P. Poignet, "A scaled bilateral teleoperation system for robotic-assisted surgery with time delay," *Journal of Intelligent & Robotic Systems*, vol. 95, no. 1, pp. 165–192, 2019.
- [9] C. Schou, J. S. Damgaard, S. Bøgh, and O. Madsen, "Human-robot interface for instructing industrial tasks using kinesthetic teaching," in *IEEE ISR 2013*. IEEE, 2013, pp. 1–6.
- [10] B. Akgun, M. Cakmak, J. W. Yoo, and A. L. Thomaz, "Trajectories and keyframes for kinesthetic teaching: A human-robot interaction perspective," in *International Conference on Human-Robot Interaction*, 2012, pp. 391–398.
- [11] F. Steinmetz, A. Montebelli, and V. Kyriki, "Simultaneous kinesthetic teaching of positional and force requirements for sequential in-contact tasks," in *International Conference on Humanoid Robots*, 2015, pp. 202–209.
- [12] Y. Kuniyoshi, M. Inaba, and H. Inoue, "Learning by Watching: Extracting reusable task knowledge from visual observation of human performance," *Transactions on Robotics and Automation*, vol. 10, no. 6, pp. 799–822, 1994.
- [13] T. Yu, C. Finn, A. Xie, S. Dasari, T. Zhang, P. Abbeel, and S. Levine, "One-shot imitation from observing humans via domain-adaptive meta-learning," *arXiv preprint arXiv:1802.01557*, 2018.
- [14] Y. Liu, A. Gupta, P. Abbeel, and S. Levine, "Imitation from observation: Learning to imitate behaviors from raw video via context translation," in *International Conference on Robotics and Automation*, 2018, pp. 1118–1125.
- [15] H. Xiong, Q. Li, Y.-C. Chen, H. Bharadhwaj, S. Sinha, and A. Garg, "Learning by watching: Physical imitation of manipulation skills from human videos," *arXiv preprint arXiv:2101.07241*, 2021.
- [16] S. Song, A. Zeng, J. Lee, and T. Funkhouser, "Grasping in the wild: Learning 6dof closed-loop grasping from low-cost demonstrations," *IEEE Robotics and Automation Letters*, vol. 5, no. 3, pp. 4978–4985, 2020.
- [17] M. Hayhoe and D. Ballard, "Eye movements in natural behavior," *Trends in Cognitive Sciences*, vol. 9, pp. 188–94, 2005.
- [18] T. Kanai, Y. Ohmura, A. Nagakubo, and Y. Kuniyoshi, "Third-party evaluation of robotic hand designs using a mechanical glove," *arXiv preprint arXiv:2109.10501*, 2021.
- [19] C. M. Bishop, "Mixture density networks," Neural Computing Research Group, Aston University, Tech. Rep., 1994.
- [20] L. Bazzani, H. Larochelle, and L. Torresani, "Recurrent mixture density network for spatiotemporal visual attention," in *International Conference on Learning Representations*, 2016.
- [21] C. Finn, X. Y. Tan, Y. Duan, T. Darrell, S. Levine, and P. Abbeel, "Deep spatial autoencoders for visuomotor learning," in *International Conference on Robotics and Automation*, 2016, pp. 512–519.
- [22] J. Pelz, M. Hayhoe, and R. Loeber, "The coordination of eye, head, and hand movements in a natural task," *Experimental Brain Research*, vol. 139, pp. 266–77, 2001.
- [23] A. Vaswani, N. Shazeer, N. Parmar, J. Uszkoreit, L. Jones, A. N. Gomez, Ł. Kaiser, and I. Polosukhin, "Attention is all you need," in *Neural Information Processing Systems*, 2017, pp. 5998–6008.
- [24] K. He, X. Zhang, S. Ren, and J. Sun, "Deep residual learning for image recognition," in *Conference on Computer Vision and Pattern Recognition*, 2016, pp. 770–778.
- [25] J. Sijs, F. Liefhebber, and G. W. R. Romer, "Combined position & force control for a robotic manipulator," in *International Conference on Rehabilitation Robotics*, 2007, pp. 106–111.
- [26] L. Liu, H. Jiang, P. He, W. Chen, X. Liu, J. Gao, and J. Han, "On the variance of the adaptive learning rate and beyond," in *International Conference on Learning Representations*, 2020, pp. 1–14.